



Article

Ceramics Based on Sodium Rhenanite CaNaPO_4 , Obtained via Firing of Composite Cement-Salt Stone

Otabek Toshev ^{1,*}, Tatiana Safronova ^{1,2}, Gilyana Kazakova ¹, Tatiana Shatalova ^{1,2}, Olga Boytsova ^{1,2}, Yulia Lukina ^{3,4} and Sergej Sivkov ⁴

¹ Department of Materials Science, Lomonosov Moscow State University, Building, 73, Leninskie Gory, 1, 119991 Moscow, Russia

² Department of Chemistry, Lomonosov Moscow State University, Building, 3, Leninskie Gory, 1, 119991 Moscow, Russia

³ National Medical Research Center for Traumatology and Orthopedics Named after N.N. Priorov, Priorova 10, 127299 Moscow, Russia

⁴ Faculty of Technology of Inorganic Substances and High-Temperature Materials, Mendeleev University of Chemical Technology of Russia, Miusskaya pl. 9, 125047 Moscow, Russia

* Correspondence: toshevou@my.msu.ru; Tel.: +7-977-522-50-62

Abstract: Ceramics based on rhenanite CaNaPO_4 with density of 0.94 g/cm^3 and compressive strength of 10.3 MPa was obtained via firing at 900°C of composite cement-salt stone prepared from a hardening powder mixture of calcium citrate tetrahydrate $\text{Ca}_3(\text{C}_6\text{H}_5\text{O}_7)_2 \cdot 4\text{H}_2\text{O}$ and sodium dihydrogen phosphate NaH_2PO_4 . The phase composition of the obtained samples of cement-salt stone was represented by monetite CaHPO_4 , unreacted sodium dihydrogen phosphate and calcium citrate tetrahydrate. According to the XRD data, the phase composition of the ceramic samples after annealing in the temperature range of $500\text{--}700^\circ\text{C}$ was mainly represented by the $\beta\text{-CaNaPO}_4$ phase. It was found that after an annealing at temperature of 900°C , the phase composition of ceramics was presented with the only phase of $\beta\text{-CaNaPO}_4$. It was demonstrated that an increase in the annealing temperature led to an increase in the grain size from $1 \mu\text{m}$ after annealing at 500°C to $5 \mu\text{m}$ after annealing at 900°C . Obtained ceramic material based on CaNaPO_4 could be important for regenerative treatments of bone tissue defects.

Keywords: dihydrogen phosphate; calcium citrate tetrahydrate; hardening; cement-salt stone; heterophase reaction; rhenanite



Citation: Toshev, O.; Safronova, T.; Kazakova, G.; Shatalova, T.; Boytsova, O.; Lukina, Y.; Sivkov, S. Ceramics Based on Sodium Rhenanite CaNaPO_4 , Obtained via Firing of Composite Cement-Salt Stone. *J. Compos. Sci.* **2022**, *6*, 314. <https://doi.org/10.3390/jcs6100314>

Academic Editor:
Francesco Tornabene

Received: 1 August 2022

Accepted: 8 October 2022

Published: 14 October 2022

Publisher's Note: MDPI stays neutral with regard to jurisdictional claims in published maps and institutional affiliations.



Copyright: © 2022 by the authors. Licensee MDPI, Basel, Switzerland. This article is an open access article distributed under the terms and conditions of the Creative Commons Attribution (CC BY) license (<https://creativecommons.org/licenses/by/4.0/>).

1. Introduction

One of the important areas of modern inorganic materials science is the development of biomaterials based on calcium phosphates that could be used to replace or treat damaged bone tissue [1,2]. Ideally, the implant should gradually dissolve in the body's environment, while performing its supporting functions, and new bone tissue should form in its place. In this regard, the key characteristic of the material is its ability to resorb in the body's environment. The traditionally used hydroxyapatite (HA), $\text{Ca}_{10}(\text{PO}_4)_6(\text{OH})_2$, has the lowest solubility among calcium phosphates [3]. In the case of a regenerative approach to the treatment of bone tissue, bioresorbable phases are introduced into the composition of materials for bone implants which, compared to HA, have greater resorption, namely tricalcium phosphate $\beta\text{-Ca}_3(\text{PO}_4)_2$ ($\text{Ca}/\text{P} = 1.5$) [4–6], calcium pyrophosphate $\text{Ca}_2\text{P}_2\text{O}_7$ ($\text{Ca}/\text{P} = 1$) [7–9], tromelite $\text{Ca}_4\text{P}_6\text{O}_{19}$ ($\text{Ca}/\text{P} = 0.66$) [10,11], calcium polyphosphate $\text{Ca}(\text{PO}_3)_2$ ($\text{Ca}/\text{P} = 0.5$) [12], Na-substituted tricalcium phosphate $\text{Ca}_{10}\text{Na}(\text{PO}_4)_7$, K-substituted tricalcium phosphate $\text{Ca}_{10}\text{K}(\text{PO}_4)_7$, sodium rhenanite CaNaPO_4 , and potassium rhenanite CaKPO_4 [13,14]. A necessary element of any strategy for improving the solubility of a compound with an ionic nature of the chemical bond is lowering the energy of the crystal lattice. Consistent implementation of this approach leads to two directions of

increasing the resorption of calcium phosphate materials, as follows: (a) transition to calcium phosphates with a Ca/P ratio lower than that of HA; (b) modification of the chemical composition associated with the replacement of the Ca^{2+} cation in the phosphate structure.

Thus, ceramics based on rhenanite CaMPO_4 , where (M = Na or K) are of great interest for different biomedical applications [15,16].

A known method for producing rhenanite CaNaPO_4 , is the crystallization of glass in the system $\text{SiO}_2\text{-Al}_2\text{O}_3\text{-Na}_2\text{O-K}_2\text{O-P}_2\text{O}_5\text{-F}$ [17] or in $\text{SiO}_2\text{-CaO-Na}_2\text{O-P}_2\text{O}_5\text{-F-K}_2\text{O}$ [18]. However, this method does not allow to obtain rhenanite CaNaPO_4 as the only phase.

There is a method of processing phosphate ores using sodium carbonate or potassium chloride at temperatures of 300–900 °C, when the formation of rhenanite CaNaPO_4 occurs only when the phosphate stone interacts with sodium carbonate [19]. This method is not suitable for the synthesis of rhenanite CaNaPO_4 for medical uses.

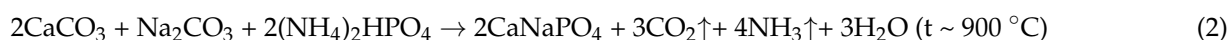
It is well-known that rhenanite CaNaPO_4 powder can be synthesized by heating a mixture of Na_2CO_3 and $\text{Ca}_2\text{P}_2\text{O}_7$ at 1000 °C for 10 h [20]. The solid-phase synthesis of rhenanite CaNaPO_4 carried out in this way, as is typical for any solid-phase synthesis, gives a powder with low sintering activity which will require higher temperatures to form ceramics based on it.

The ref. [21] shows a method for obtaining a material based on rhenanite CaNaPO_4 from a charge containing sodium salt (sodium bicarbonate NaHCO_3) and calcium phosphate – monetite CaHPO_4 . This process includes pressing the initial charge and firing at 1300 °C for 16 h. The main disadvantages of this method are the high temperature of the reaction and duration of the synthesis.

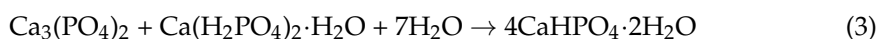
Rhenanites are very widely used to obtain phosphate fertilizers. Here, the “Rhenania process” should be mentioned, which is a well-known procedure used in the fertilizer industry to obtain soluble phosphate materials [22]. In this process, the natural mineral fluorapatite $\text{Ca}_5(\text{PO}_4)_3\text{F}$ is mixed with soda Na_2CO_3 and silicon dioxide SiO_2 while the molar ratio of $\text{Na}_2\text{CO}_3 / \text{P}_2\text{O}_5$ is fixed at 1.0 (Equation (1)). The SiO_2 is added to prevent the occurrence of free CaO in the sintered product. These powder mixtures are then crushed and calcined in a rotary kiln at around 1000–1200 °C for several hours. Rhenanite, a highly soluble CaNaPO_4 , is the major phase in the final product of the Rhenania process [22].



Furthermore, CaNaPO_4 can also be obtained via firing a mixture of CaO, H_3PO_4 and Na_2CO_3 [22] at 1100 °C. Other starting components can be used for rhenanite CaNaPO_4 preparation (Equation (2)):



Alternatively, sodium rhenanite CaNaPO_4 can be obtained by cement technology with subsequent firing. The work [23] shows a method for obtaining CaNaPO_4 from brushite cement, prepared by the reaction of β -tricalcium phosphate, monocalcium phosphate monohydrate (Equation (3)), and a highly alkaline bioactive glass (composition (wt.%): $\text{SiO}_2\text{-50, Na}_2\text{O-25, CaO-20, P}_2\text{O}_5\text{-5}$).



After mixing brushite with bioactive glass, firing was carried out at high temperatures. With an increase in the temperature to 700–800 degrees, CaNaPO_4 , and $\beta\text{-Ca}_3(\text{PO}_4)_2$ phases were obtained, which indicates that the transition of bioactive glass to a viscoplastic state has occurred. The formation of the CaNaPO_4 phase occurs due to thermochemical interactions between Na_2O and CaO from the glass matrix and $\beta\text{-Ca}_2\text{P}_2\text{O}_7$.

Therefore, the aim of this work was to obtain bioresorbable ceramics based on rhenanite CaNaPO_4 by firing of a composite cement-salt stone prepared from powder mixture of calcium citrate $\text{Ca}_3(\text{C}_6\text{H}_5\text{O}_7)_2 \cdot 4\text{H}_2\text{O}$ and sodium dihydrogen phosphate NaH_2PO_4 .

2. Materials and Methods

2.1. Initial Reagents and Synthesis

Calcium citrate tetrahydrate $\text{Ca}_3(\text{C}_6\text{H}_5\text{O}_7)_2 \cdot 4\text{H}_2\text{O}$ (CAS No. 5785-44-4, puriss. p.a. $\geq 85\%$) and sodium dihydrogen phosphate NaH_2PO_4 (CAS No. 7558-80-7, puriss. $\geq 99\%$) were purchased from Sigma Aldrich.

2.2. Preparation of the Sodium Rhenanite Ceramics

The following Equation (4) was used to calculate the composition of the powder mixture:



The initial mixture, consisted of powders of calcium citrate tetrahydrate $\text{Ca}_3(\text{C}_6\text{H}_5\text{O}_7)_2 \cdot 4\text{H}_2\text{O}$ and sodium dihydrogen phosphate NaH_2PO_4 , were used in a molar ratio corresponding to Equation (4), which were previously homogenized in a planetary mill in an acetone medium for 15 min. The resulting powder mixture was mixed with water at a water/solid ratio (W/T) = 0.5. The resulting paste dough was mixed in a porcelain bowl for 30 s. The latex mold with sizes of $10 \times 10 \times 30$ mm was filled with prepared paste and left to harden in air for a day. The cement-salt stone samples formed as a result of hardening was fired for 2 h in the range of 500–900 °C.

2.3. Characterization

2.3.1. XRD

Here, X-Ray diffraction (XRD) analysis was conducted using a Rigaku D/Max-2500 (Rigaku, Tokyo, Japan) with a rotating anode (Cu-K α radiation), with an angle interval (2Θ) of 2–70°. Phase analysis was performed using the ICDD PDF2 database [24].

2.3.2. SEM

The microstructure of the ceramic materials was studied using a LEO SUPRA 50VP (Carl Zeiss, Jena, Germany) scanning electron microscope (SEM) with an acceleration voltage of 21 kV. The images were recorded using an Everhart–Thornley secondary electron detector (SE2). The SEM specimens were prepared by depositing a small amount of the samples onto an aluminum substrate followed by coating the surface with a chromium layer to avoid the charging effects. The surface of the cement-stone and ceramic samples was coated with a layer of chromium (up to 15 nm).

2.3.3. Thermal Analysis

Thermal analysis (TA) was carried out using a NETZSCH STA 409 PC Luxx thermal analyzer (NETZSCH, Selb, Germany), in the temperature range of 40–1000 °C. The composition of the gas phase formed upon decomposition of samples was studied using a QMS 403C Aëolos quadrupole mass spectrometer (NETZSCH, Germany) coupled to the NETZSCH STA 409 PC Luxx thermal analyzer. Mass spectra (MS) were recorded for $m/Z = 18$ (H_2O), as well as for $m/Z = 44$ (CO_2).

2.3.4. Determination of Strength Properties

The bending and compressive strengths of ceramic samples in form of balks were determined using universal testing machines LFV 10-T50 (Switzerland) and P-05, respectively.

3. Results and Discussion

The XRD patterns of the initial components and cement-salt stone based on calcium citrate and sodium dihydrogen phosphate are shown in Figure 1.

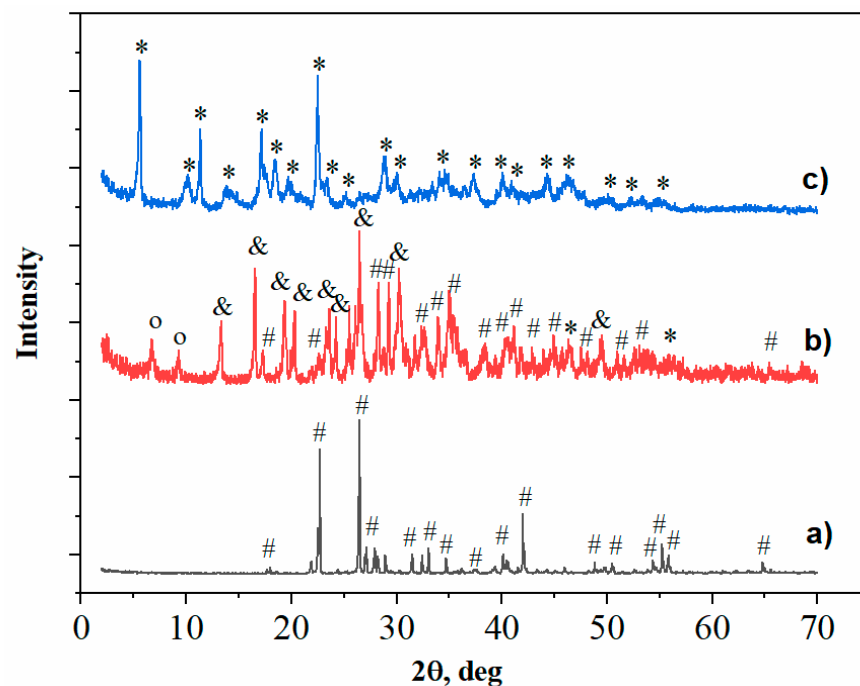
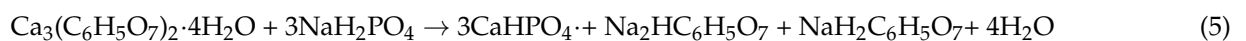


Figure 1. The XRD spectra of the initial components, as follows: sodium dihydrogen phosphate (a), calcium citrate tetrahydrate (c), and cement-salt stone based on calcium citrate tetrahydrate and sodium dihydrogen phosphate (b). Symbols are as follows: #— NaH_2PO_4 (PDF 70-954); *— $\text{Ca}_3(\text{C}_6\text{H}_5\text{O}_7)_2 \cdot 4\text{H}_2\text{O}$ (PDF 28-2003); o—non-identified reflexes; &— CaHPO_4 (PDF 70-360).

The Equation (5) reflects the reaction of phase composition of cement-salt stone formation:



According to the XRD data (Figure 1), the main phases in the cement-salt stone based on calcium citrate tetrahydrate and sodium dihydrogen phosphate are monetite CaHPO_4 , unreacted sodium dihydrogen phosphate, and calcium citrate tetrahydrate. The presence of unreacted components shows that the reaction has not been fully completed in the conditions given here. There are also peaks that probably correspond to the acidic calcium citrate salts, such as $\text{Na}_2\text{HC}_6\text{H}_5\text{O}_7$ and $\text{NaH}_2\text{C}_6\text{H}_5\text{O}_7$.

The microstructure studies of the cement-salt stone support the results of the XRD data. The micrograph of the sample demonstrated in Figure 2 shows small crystals of monetite CaHPO_4 with plate-like morphology and particles of sodium dihydrogen phosphate NaH_2PO_4 of spheric shapes. The CaHPO_4 crystals are most likely formed on the surface of the less soluble calcium citrate. The CaHPO_4 crystals have a size of less than $2 \mu\text{m}$ due to the action of $\text{C}_6\text{H}_5\text{O}_7^{3-}$ which slows down the reaction and inhibits the growth of calcium hydrogen phosphate crystals.

According to the simultaneous thermal analysis (Figure 3), the total weight loss of the powder mixture when heated to 1000°C was 44 %.

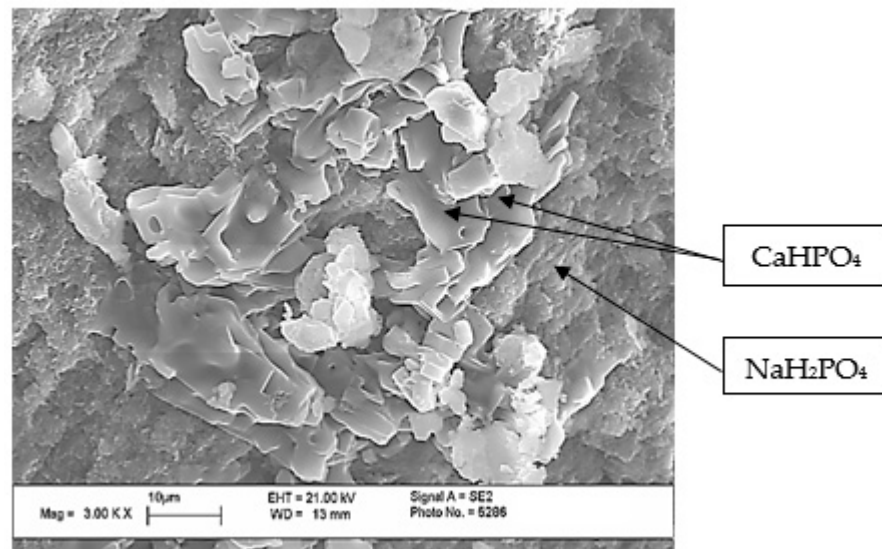


Figure 2. The SEM image of cement-salt stone based on calcium citrate tetrahydrate and sodium dihydrogen phosphate.

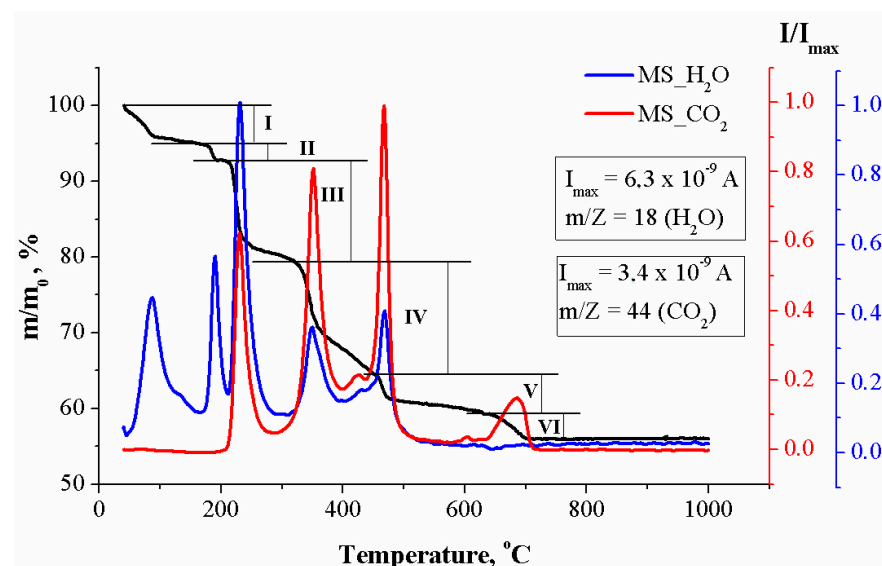
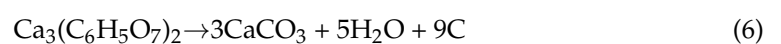


Figure 3. Thermal analysis of the cement-salt stone based on powder mixture of calcium citrate tetrahydrate and sodium dihydrogen phosphate: powder mass versus temperature upon heating (**black curve**), mass spectra for evolving gases with $m/Z = 18$ (H_2O) (**blue curve**), and for $m/Z = 44$ (CO_2) (**red curve**).

Three peaks can be observed on the mass spectrum curve for $m/Z = 18$ (H_2O) in the range of 50–300 °C. In this temperature range, thermal decomposition of calcium citrate tetrahydrate $\text{Ca}_3(\text{C}_6\text{H}_5\text{O}_7)_2 \cdot 4\text{H}_2\text{O}$ with the formation of anhydrous calcium citrate $\text{Ca}_3(\text{C}_6\text{H}_5\text{O}_7)_2$ is possible. On the mass spectrum curve for $m/Z = 44$, there is a peak in the range of 435–495 °C, reflecting the release of CO_2 . Thermal decomposition of anhydrous calcium citrate $\text{Ca}_3(\text{C}_6\text{H}_5\text{O}_7)_2$ with the formation of calcium carbonate CaCO_3 occurs with heat release according to the following Equation (6):

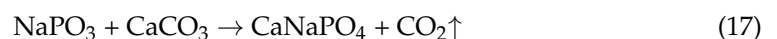
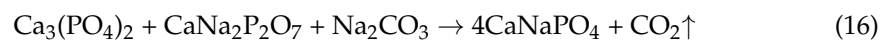
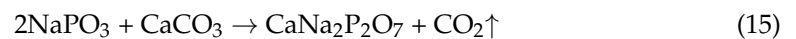
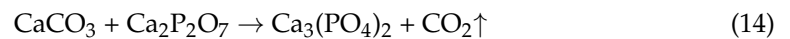
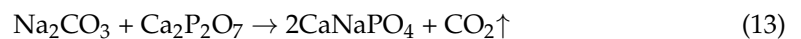
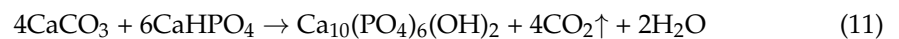
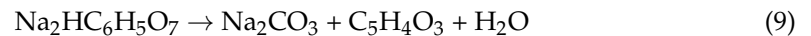


The carbon formed as a result of this transformation (Equation (6)) could not remain in elemental form at such a high temperature (above 340 °C), especially in the presence of atmospheric oxygen. Therefore, it must have turned into CO and/or CO_2 . In the temper-

ature range of 450–650 °C, the following process is observed: calcium carbonate CaCO_3 transforms into calcium oxide and CO_2 , as follows (Equation (7)):



During the heat treatment, the products obtained during the acid-base reaction thermally decomposed, and products of thermal decomposition interacted with each other to form ceramics. The processes taking place during heating can be described by the following equations:



During the heat treatment of cement-salt stone at temperatures of 500 and 700 °C (Figure 4), in addition to the target phase $\beta\text{-CaNaPO}_4$, hydroxyapatite $\text{Ca}_{10}(\text{PO}_4)_6(\text{OH})_2$ was formed. This phase was formed due to the interaction of monetite CaHPO_4 with calcium carbonate CaCO_3 (Equation (11)) which was the product of the calcium citrate $\text{Ca}_3(\text{C}_6\text{H}_5\text{O}_7)_2$ decomposition (Equation (6)). At 700 °C, in addition to $\beta\text{-CaNaPO}_4$ and $\text{Ca}_{10}(\text{PO}_4)_6(\text{OH})_2$, phases of double calcium-sodium pyrophosphate $\text{CaNa}_2\text{P}_2\text{O}_7$ and $\beta\text{-Ca}_3(\text{PO}_4)_2$ phases were formed. The formation of the $\text{CaNa}_2\text{P}_2\text{O}_7$ phase was due to the interaction of the NaPO_3 melt with calcium oxide CaCO_3 (Equation (15)). The $\beta\text{-Ca}_3(\text{PO}_4)_2$ phase was formed as a result of the interaction of CaCO_3 with $\text{Ca}_2\text{P}_2\text{O}_7$ (Equation (14)). At 900 °C, only the target phase $\beta\text{-CaNaPO}_4$ was found.

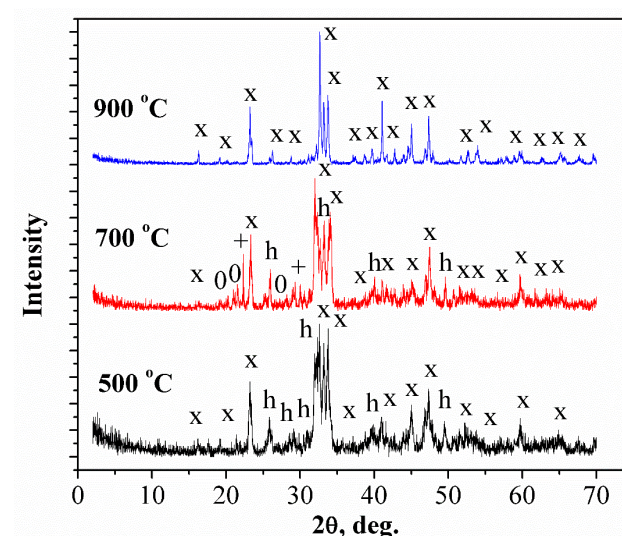


Figure 4. The XRD of ceramic samples based on cement-salt stone prepared from powder mixture of calcium citrate tetrahydrate and sodium dihydrogen phosphate in the temperature range of 500–900 °C. x— $\beta\text{-CaNaPO}_4$ (PDF 29-1193); h— $\text{Ca}_{10}(\text{PO}_4)_6(\text{OH})_2$ (PDF 74-565); +— $\beta\text{-Ca}_3(\text{PO}_4)_2$ (PDF 9-169); 0— $\text{CaNa}_2\text{P}_2\text{O}_7$ (PDF 48-557).

The geometric density of ceramic materials is shown in Figure 5. After firing at 500 °C, the density of ceramic samples was 0.56 g/cm³. The density of ceramics has decreased compared to the density of cement-salt stone. The decrease in the density of the samples was due to a decrease in the mass of the sample, because of the decomposition of the components of the cement-salt stone during heating (Figure 6). With an increase in firing temperature from 700 °C to 900 °C, the ceramic density increased from 0.68 g/cm³ to 0.94 g/cm³ or from 21.8 % to 30.2% relatively to the density of β -CaNaPO₄ equal to 3.11 g/cm³ (Figure 7). The shrinkage of the samples was 2.7% and 17.8% at 500 °C and 900 °C, respectively.

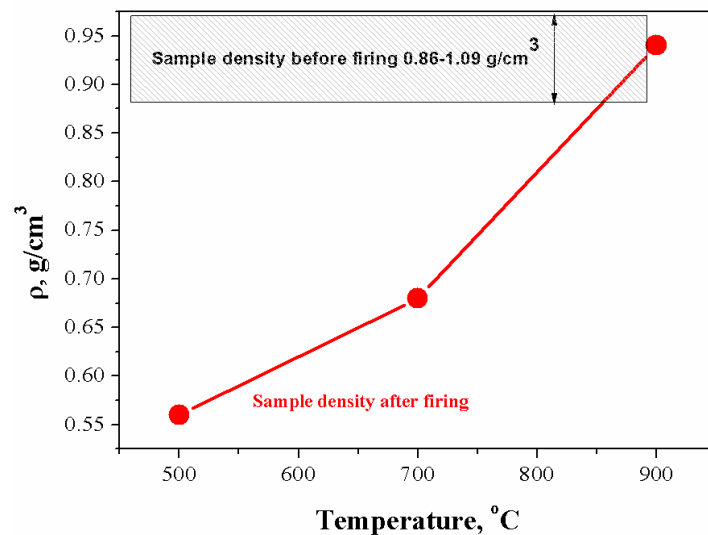


Figure 5. Geometric density of ceramic samples, obtained by annealing of cement-salt stone in the temperature range of 500–900 °C.

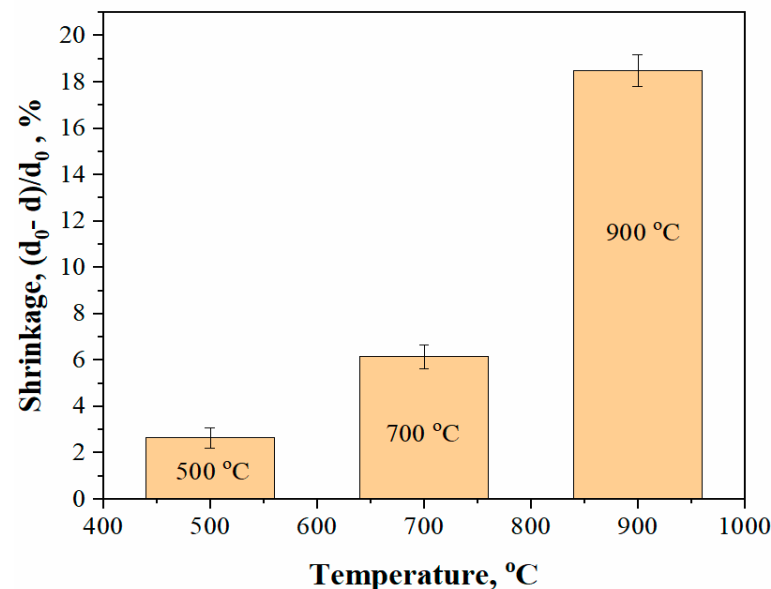


Figure 6. Shrinkage of ceramic samples, obtained by annealing of cement-salt stone in the temperature range of 500–900 °C.

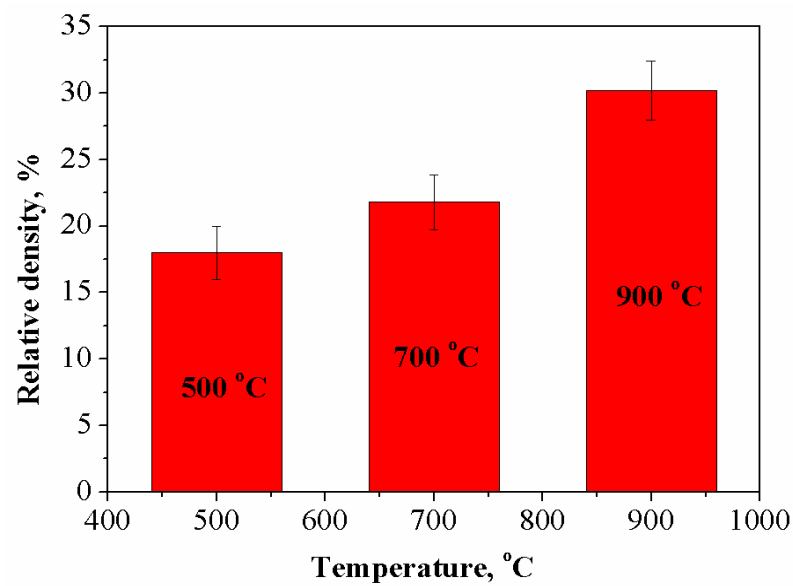


Figure 7. Relative density of ceramic samples, obtained via annealing of cement-salt stone in the temperature range of 500–900 °C.

The SEM images of the samples shown in Figure 8 clearly demonstrate that Na-rhenanite crystals grow from 1 to 5 µm substantially as the firing temperature increases from 700 °C to 900 °C.

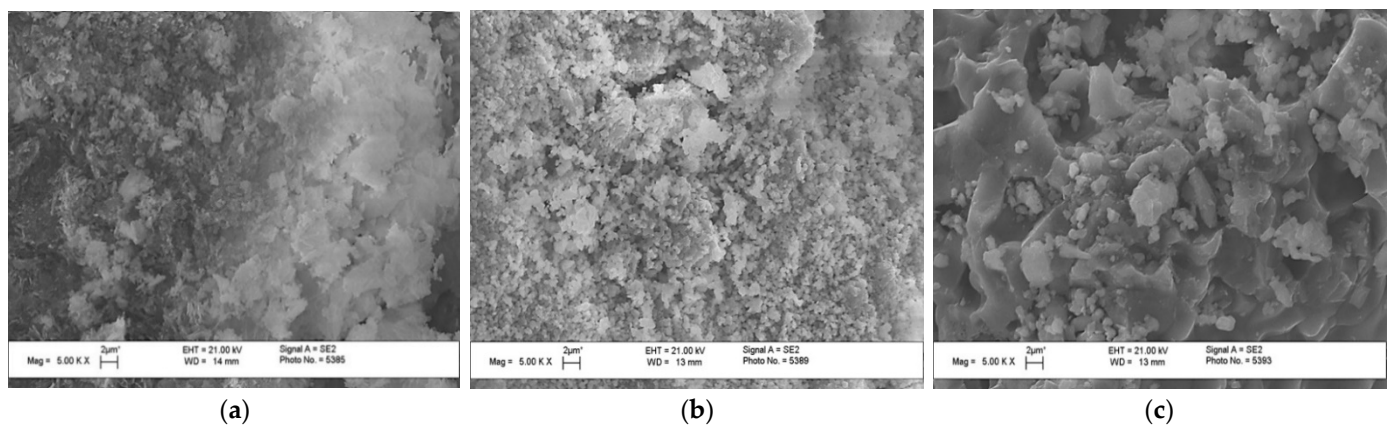


Figure 8. The SEM images of ceramic samples based on cement-salt stone prepared from powder mixture of calcium citrate tetrahydrate and sodium dihydrogen phosphate, after firing at temperatures of 500 °C (a), 700 °C (b), and 900 °C (c).

Figure 9 shows the temperature dependence of compressive and bending strengths of ceramic materials. The compressive strength of ceramic samples (Figure 9) increase from 3.5 to 10.3 MPa with increasing temperature from 500 °C to 900 °C, This compressive strength increasement is associated with the process of liquid-phase sintering, leading to the formation of more durable contacts between grains.

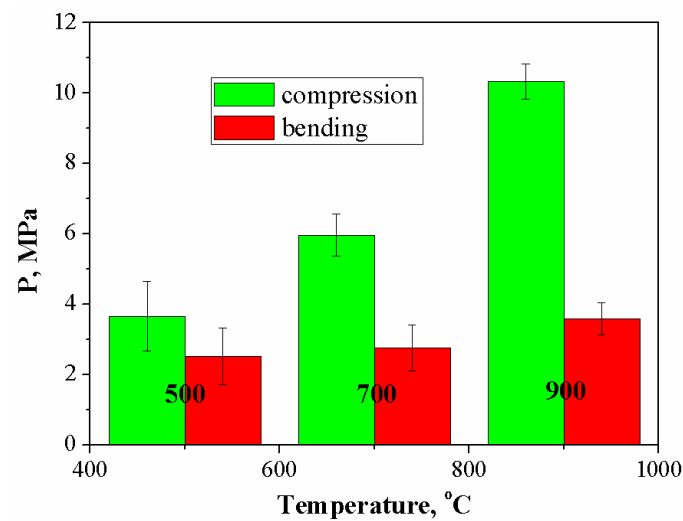


Figure 9. The compressive and bending strengths of the ceramic samples based on cement-salt stone prepared from powder mixture of citrate tetrahydrate and sodium dihydrogen phosphate after annealing at temperature range of 500–900 °C.

4. Conclusions

In the present work, an approach to obtaining bioresorbable ceramics with a phase composition represented by β -CaNaPO₄ was described. This approach involved the preparation of a powder mixture with a given molar ratio of Na:Ca:P = 1, which was capable of entering into a chemical reaction; molding samples of cement-salt stone; and firing samples of cement-salt stone to obtain ceramics.

Samples of cement-salt stone were prepared from a powder mixture with a molar ratio of Na:Ca:P = 1, including calcium citrate tetrahydrate $\text{Ca}_3(\text{C}_6\text{H}_5\text{O}_7)_2 \cdot 4\text{H}_2\text{O}$ and sodium dihydrogen phosphate NaH_2PO_4 . The phase composition of cement-salt stone samples based on $\text{Ca}_3(\text{C}_6\text{H}_5\text{O}_7)_2 \cdot 4\text{H}_2\text{O}$ and NaH_2PO_4 was represented mainly by monetite CaHPO_4 , as well as unreacted NaH_2PO_4 and $\text{Ca}_3(\text{C}_6\text{H}_5\text{O}_7)_2 \cdot 4\text{H}_2\text{O}$. Heat treatment of the obtained cement-salt stone at a temperature of 500 °C led to the formation of β -CaNaPO₄ and $\text{Ca}_{10}(\text{PO}_4)_6(\text{OH})_2$ phases. At 700 °C, in addition to β -CaNaPO₄ and $\text{Ca}_{10}(\text{PO}_4)_6(\text{OH})_2$, the phases of double calcium-sodium pyrophosphate $\text{Na}_2\text{CaP}_2\text{O}_7$ and β -Ca₃(PO₄)₂ were formed. According to the XRD data, after firing at 900 °C, the resulting ceramics contained the only β -CaNaPO₄ phase. It was shown that, as the temperature increased, the shrinkage and density of ceramic samples increased. Thus, ceramic material with density of 0.94 g/cm³ developed here consisting of biocompatible and bioresorbable β -CaNaPO₄ phase can be used in regenerative methods for the treatment of bone tissue defects.

Author Contributions: Conceptualization, O.T. and T.S. (Tatiana Safronova); Methodology, T.S. (Tatiana Safronova); Investigation, O.T., T.S. (Tatiana Safronova), T.S. (Tatiana Shatalova), O.B., G.K., Y.L. and S.S.; Visualization, O.T., O.B. and T.S. (Tatiana Shatalova); Writing—original draft, O.T. and T.S. (Tatiana Safronova); Writing—review & editing, O.T.; Supervision, T.S. (Tatiana Safronova); Project administration, T.S. (Tatiana Safronova). All authors have read and agreed to the published version of the manuscript.

Funding: This work was carried out with financial support from the Russian Foundation for Basic Research (RFBR) (grant No. 20-03-00550).

Data Availability Statement: Not applicable.

Acknowledgments: The research was carried out using the equipment of MSU Shared Research Equipment Center “Technologies for obtaining new nanostructured materials and their complex study” and purchased by MSU in the frame of the Equipment Renovation Program (National Project “Science”) and in the frame of the MSU Program of Development.

Conflicts of Interest: The authors declare that they have no known competing financial interests or personal relationships that could have appeared to influence the work reported in this paper.

References

1. Tavoni, M.; Dapporto, M.; Tampieri, A.; Sprio, S. Bioactive calcium phosphate-based composites for bone regeneration. *J. Compos. Sci.* **2021**, *5*, 227. [\[CrossRef\]](#)
2. Makeeva, I.M.; Poliakova, M.A.; Doroshina, V.I.; Sokhova, I.A.; Arakelian, M.G.; Makeeva, M.K. Efficiency of paste and suspension with nano-hydroxyapatite on the sensitivity of teeth with gingival recession. *Stomatologiya* **2018**, *97*, 23–27. [\[CrossRef\]](#) [\[PubMed\]](#)
3. Kanazawa, T. *Inorganic Phosphate Materials*; Elsevier Science Ltd.: Oxford, UK, 1989; 306p.
4. Evdokimov, P.V.; Tikhonova, S.A.; Kiseleva, A.K.; Filippov, Y.Y.; Novoseletskaia, E.S.; Efimenko, A.Y.; Putlayev, V.I. Effect of the pore size on the biological activity of β - $\text{Ca}_3(\text{PO}_4)_2$ -based resorbable macroporous ceramic materials obtained by photopolymerization. *Russ. J. Inorg. Chem.* **2021**, *66*, 1609–1615. [\[CrossRef\]](#)
5. Bohner, M.; Santoni, B.L.G.; Dobelin, N. β -tricalcium phosphate for bone substitution: Synthesis and properties. *Acta Biomater.* **2020**, *113*, 23–41. [\[CrossRef\]](#) [\[PubMed\]](#)
6. Eliaz, N.; Metoki, N. Calcium phosphate bioceramics: A review of their history, structure, properties, coating technologies and biomedical applications. *Materials* **2017**, *10*, 334. [\[CrossRef\]](#) [\[PubMed\]](#)
7. Safronova, T.; Kiselev, A.; Selezneva, I.; Shatalova, T.; Lukina, Y.; Filippov, Y.; Toshev, O.; Tihonova, S.; Antonova, O.; Knotko, A. Bioceramics Based on β -Calcium Pyrophosphate. *Materials* **2022**, *15*, 3105. [\[CrossRef\]](#)
8. Toshev, O.; Safronova, T.; Kaimonov, M.; Shatalova, T.; Klimashina, E.; Lukina, Y.; Malyutin, K.; Sivkov, S. Biocompatibility of ceramic materials in $\text{Ca}_2\text{P}_2\text{O}_7$ – $\text{Ca}(\text{PO}_3)_2$ system obtained via heat treatment of cement-salt stone. *Ceramics* **2022**, *5*, 516–532. [\[CrossRef\]](#)
9. Lee, J.H.; Chang, B.-S.; Jeung, U.-O.; Park, K.-W.; Kim, M.-S.; Lee, C.-K. The first clinical trial of beta-calcium pyrophosphate as a novel bone graft extender in instrumented posterolateral lumbar fusion. *Clin. Orthop. Surg.* **2011**, *3*, 238. [\[CrossRef\]](#) [\[PubMed\]](#)
10. Hoppe, H.A. Synthesis, crystal structure, and vibrational spectra of $\text{Ca}_4\text{P}_6\text{O}_{19}$ (Tromelite)? A catena? Hexaphosphate. *Z. Anorg. Allg. Chem.* **2005**, *631*, 1272–1276. [\[CrossRef\]](#)
11. Safronova, T.V.; Mukhin, E.A.; Putlyaev, V.I.; Knotko, A.V.; Evdokimov, P.V.; Shatalova, T.B.; Filippov, Y.Y.; Sidorov, E.A.; Karpushkin, E.A. Amorphous calcium phosphate powder synthesized from calcium acetate and polyphosphoric acid for bioceramics application. *Ceram. Int.* **2017**, *43*, 1310–1317. [\[CrossRef\]](#)
12. Yuan, Y.; Yuan, Q.; Wu, C.; Ding, Z.; Wang, X.; Li, G.; Gu, Z.; Li, L.; Xie, H. Enhanced osteoconductivity and osseointegration in calcium polyphosphate bioceramic scaffold via lithium doping for bone regeneration. *ACS Biomater. Sci. Eng.* **2019**, *5*, 5872–5880. [\[CrossRef\]](#) [\[PubMed\]](#)
13. Evdokimov, P.V.; Putlyaev, V.I.; Ivanov, V.K.; Garshev, A.V.; Shatalova, T.B.; Orlov, N.K.; Klimashina, E.S.; Safronova, T.V. Phase equilibria in the tricalcium phosphate–mixed calcium sodium (potassium) phosphate systems. *Russ. J. Inorg. Chem.* **2014**, *59*, 1219–1227. [\[CrossRef\]](#)
14. Orlov, N.K.; Putlayev, V.I.; Evdokimov, P.V.; Safronova, T.V.; Garshev, A.V.; Milkin, P.A. Composite Bioceramics Engineering Based on Analysis of Phase Equilibria in the $\text{Ca}_3(\text{PO}_4)_2$ – CaNaPO_4 – CaKPO_4 system. *Inorg. Mater.* **2019**, *55*, 516–523. [\[CrossRef\]](#)
15. Orlov, N.K.; Kiseleva, A.K.; Milkin, P.A.; Evdokimov, P.V.; Putlayev, V.I.; Günster, J. Potentialities of Reaction Sintering in the Fabrication of High-Strength Macroporous Ceramics Based on Substituted Calcium Phosphate. *Inorg. Mater.* **2020**, *56*, 1298–1306. [\[CrossRef\]](#)
16. Orlov, N.; Kiseleva, A.; Milkin, P.; Evdokimov, P.; Putlayev, V.; Günster, J.; Biesuz, M.; Sglavod, V.M.; Tyablikov, A. Sintering of mixed Ca–K–Na phosphates: Spark plasma sintering vs flash-sintering. *Open Ceramics* **2021**, *5*, 100072. [\[CrossRef\]](#)
17. Holland, W.; Rheinberger, V.; Wegner, S.; Frank, M. Needle-like apatite-leucite glass-ceramic as a base material for the veneering of metal restorations in dentistry. *J. Mater. Sci. Mater. Med.* **2000**, *11*, 11–17. [\[CrossRef\]](#) [\[PubMed\]](#)
18. Apel, E.; Holland, W.; Rheinberger, V. Bioactive Rhenanite Glass. Ceramic. Patent US No. 7,074,730, 11 July 2006.
19. Rautaray, H.K.; Dash, R.N.; Mohanty, S.K. Phosphorus supplying power of some thermally promoted reaction products of phosphate rocks. *Fertil. Res.* **1995**, *41*, 67–75. [\[CrossRef\]](#)
20. Suchanek, W.; Yashima, M.; Kakihana, M.; Yoshimura, M. β -Rhenanite (β - NaCaPO_4) as weak interphase for hydroxyapatite ceramics. *J. Eur. Ceram. Soc.* **1989**, *18*, 1923–1929. [\[CrossRef\]](#)
21. Ramselaar, M.M.A.; Van Mullem, P.J.; Kalk, W.; Driessens, F.C.M.; Dewijn, J.R.; Stols, A.L.H. In vivo reactions to particulate rhenanite and particulate hydroxyapatite after implantation in tooth sockets. *J. Mater. Sci. Mater. Med.* **1993**, *4*, 311–317. [\[CrossRef\]](#)
22. Glasser, F.P.; Gunawardane, R.P. Fertilizer Material from Apatite. U.S. Patent No. 4,363,650, 14 December 1982.
23. Svetskaya, N.V.; Lukina, Y.S.; Larionov, D.S.; Andreev, D.V.; Sivkov, S.P. 3D-matrix based on bioactive glass and calcium phosphates with controllable resorption rate for bone tissue replacement. *Glass Ceram.* **2017**, *73*, 342–347. [\[CrossRef\]](#)
24. ICDD. *International Centre for Diffraction Data*; Kabekkodu, S., Ed.; PDF-4+ 2010 (Database); ICDD: Newtown Square, PA, USA, 2010. Available online: <https://www.icdd.com/pdf-2/> (accessed on 20 February 2022).